Emission and oxidation of methane in a meromictic, eutrophic and temperate lake (Dendre, Belgium)

Fleur A.E. Roland [a, *], François Darchambeau [a], Cédric Morana [b], Steven Bouillon [b], Alberto V. Borges [a]

[a] Chemical Oceanography Unit, Université de Liège, Belgium
[b] Department of Earth and Environmental Sciences, Katholieke Universiteit Leuven (KU Leuven), Belgium

HIGHLIGHTS

- The studied lake was meromictic and characterized by high methane, nutrients and sulfate concentrations in the water column.
- High aerobic and anaerobic methane oxidation rates were observed in the water column, and were dependent on the season.
- Anaerobic methane oxidation was linked to sulfate reduction, and potentially to nitrate reduction.
- Despite high methane oxidation rates, methane fluxes to the atmosphere were high.

ARTICLE INFO

ABSTRACT

We sampled the water column of the Dendre stone pit lake (Belgium) in spring, summer, autumn and winter. Depth profiles of several physico-chemical variables, nutrients, dissolved gases (CO_2, CH_4, N_2O), sulfate, sulfide, iron and manganese concentrations and $\delta^{13}C$-CH4 were determined. We performed incubation experiments to quantify CH_4 oxidation rates, with a focus on anaerobic CH_4 oxidation (AOM), without and with an inhibitor of sulfate reduction (molybdate). The evolution of nitrate and sulfate concentrations during the incubations was monitored. The water column was anoxic below 20 m throughout the year, and was thermally stratified in summer and autumn. High partial pressure of CO_2 and CH_4 and high concentrations of ammonium and phosphate were observed in anoxic waters. Important nitrous oxide and nitrate concentration maxima were also observed (up to 440 nmol L^{-1} and 80 μmol L^{-1}, respectively). Vertical profiles of $\delta^{13}C$-CH4 unambiguously showed the occurrence of AOM. Important AOM rates (up to 14 μmol L^{-1} d^{-1}) were observed and often co-occurred with nitrate consumption peaks, suggesting the occurrence of AOM coupled with nitrate reduction. AOM coupled with sulfate reduction also occurred, since AOM rates tended to be lower when molybdate was added. CH_4 oxidation was mostly aerobic (~80% of total oxidation) in spring and winter, and almost exclusively anaerobic in summer and autumn. Despite important CH_4 oxidation rates, the estimated CH_4 fluxes from the water surface to the atmosphere were high (mean of 732 μmol m^{-2} d^{-1} in spring, summer and autumn, and up to 12,482 μmol m^{-2} d^{-1} in winter).

© 2016 Elsevier Ltd. All rights reserved.

1. Introduction

Methane (CH_4) is known to be an important natural and anthropogenic greenhouse gas. CH_4 concentrations in the atmosphere have increased dramatically during the 20th century to reach 1850 ppb in 2015, mainly due to human activities (agriculture, waste disposal and energy extraction and production) (IPCC, 2013; Kirschke et al., 2013; NOAA, 2015). In natural environments, CH_4 is anaerobically produced by methanogenic archaea. The total CH_4 emission to the atmosphere has been estimated to 540 Tg CH_4 yr^{-1}, with a significant contribution from inland waters (Bastviken et al., 2011; Borges et al., 2015; Holgerson and Raymond, 2016). The actual amount of CH_4 produced is higher, as a significant fraction of CH_4 produced is biologically oxidized before reaching the atmosphere (Bastviken et al., 2002). CH_4 oxidation limits the flux of CH_4 to the atmosphere, and in inland waters can fuel a

microbial based food-web (Jones and Grey, 2011).

CH_4 oxidation can be performed under both aerobic and anaerobic conditions. It is now commonly assumed that anaerobic CH_4 oxidation (AOM) can occur with different final electron acceptors: sulfate (SO_4^{2-}), nitrate (NO_3^-), nitrite (NO_2^-), iron (Fe) and/or manganese (Mn) (Borrel et al., 2011). In seawater, NO_3^- concentrations are low (usually < 5 μmol L^{-1}), while SO_4^{2-} concentrations are much higher (~30 mmol L^{-1}). Also, Fe and Mn concentrations (on the order of pmol L^{-1}) in seawater are negligible compared to SO_4^{2-} concentrations. So, even if denitrification, Fe- and Mn-reduction are thermodynamically more favorable than SO_4^{2-} reduction, the latter remains the main anaerobic pathway for the degradation of organic matter in the oceans, including the degradation of CH_4. While AOM is thus generally coupled to SO_4^{2-} reduction (SDMO) in marine waters and sediments (e.g. Iversen and Jørgensen, 1985; Boetius et al., 2000; Jørgensen et al., 2001), other electron acceptors of AOM have been much less frequently studied in freshwater systems. Due to low the SO_4^{2-} concentrations usually observed in freshwaters environments, AOM is often considered to be negligible compared to aerobic CH_4 oxidation (Rudd et al., 1974). However, AOM in freshwaters can also be coupled to NO_2^- and NO_3^- reduction (NDMO), which is thermodynamically much more favorable than SDMO (free Gibs energy of -928, -765 and -17 kJ mol^{-1} CH_4, with NO_2^-, NO_3^- and SO_4^{2-} reduction, respectively; Raghoebarsing et al., 2006; Borrel et al., 2011). NDMO has been observed in experimental environments with enrichment of bacteria of interest (e.g. Ettwig et al., 2010; Hu et al., 2011; Haroon et al., 2013), or in sediments cultures with electron acceptors added (e.g. Deutzmann and Schink, 2011; á Norði and Thamdrup, 2014). Despite numerous laboratory observations, the significance of NDMO in natural environments is still largely unknown. Although AOM coupled with Fe- and Mn-reduction (FDMO and MDMO, respectively) has been proposed to occur in various freshwater environments (e.g. ferruginous lakes Matano and Kinneret; Crowe et al., 2011; Sivan et al., 2011; á Norði et al., 2013), to our knowledge no direct rate measurements have been reported in the literature.

In this study, we investigated biogeochemistry of the water column of Dendre stone pit lake (Belgium), a relatively deep (maximum depth 30 m) but small (0.032 km^2) water body in a former limestone quarry, with a focus on quantifying AOM rates and related electron acceptors. This lake was chosen to be an ideal system for studying AOM dynamics because it is known to be meromictic (waters anoxic below 20 m depth throughout the year) and rich in both organic matter (eutrophic) and sulfide (HS^-) in the anoxic layers. The lake is fed by springs at 7 and 18 m depth, providing potentially NO_3^- rich groundwater due to generalized fertilizer contamination that is common in Belgium (SPW-DGO3, 2015). We thus hypothesized that high organic matter supply and bottom layer anoxia sustain high methanogenesis rates, and that CH_4 production is removed by SDMO and/or NDMO based on occurrence of high HS^- concentrations, and potentially high NO_3^- concentrations.

2. Material and methods

2.1. Physico-chemical parameters and sampling

Sampling in the Dendre stone pit lake (50.6157°N, 3.7949°E) was carried out in spring (May 2014), summer (August 2014), winter (February 2015) and autumn (October 2015). Depth profiles of dissolved oxygen (O_2) concentrations, temperature, pH and specific conductivity were obtained with Yellow Springs Instrument 6600 V2 and Hydrolab DS5 multiparameter probes. The conductivity, pH and oxygen probes were calibrated the day before

each sampling using the protocols and standards recommended by the manufacturer.

2.2. CH_4 oxidation measurements and water column chemical analyses

At each depth of interest, duplicate samples for N_2O and CH_4 concentration analyses were collected in 60 mL glass serum bottles from a Niskin bottle through a silicon tube connected to the outlet, left to overflow, poisoned with 200 μL of a saturated $HgCl_2$ solution and immediately sealed with butyl stoppers and aluminium caps. Ten other bottles per depth were incubated in the dark and constant temperature (close to in-situ temperature): five of them received 250 μl of a solution of molybdate (1 mol L^{-1}, hence a final concentration of 4 mmol L^{-1}), an inhibitor of sulfur-reducing bacteria and five received no treatment. The biological activity of two incubated bottles (one from each treatment) was stopped at 12, 24, 48, 72 and 96 h by the addition of a saturated 200 μl $HgCl_2$ solution. CH_4 and N_2O concentrations were determined via the headspace equilibration technique (20 mL N_2 headspace in 60 mL serum bottles) and measured by gas chromatography (GC) with electron capture detection (ECD) for N_2O and with flame ionization detection (FID) for CH_4 (Weiss, 1981). The SRI 8610C GC-ECD-FID was calibrated with certified CH_4:CO_2:N_2O:N_2 mixtures (Air Liquide, Belgium) of 1, 10, 30 and 509 ppm CH_4 and of 0.2, 2.0 and 6.0 ppm N_2O. Concentrations were computed using the solubility coefficients of Yamamoto et al. (1976) and Weiss and Price (1980), for CH_4 and N_2O, respectively. The precision of measurements was $\pm3.9\%$ and $\pm3.2\%$ for CH_4 and N_2O, respectively. CH_4 oxidation rates were calculated based on the decrease of CH_4 concentrations in the incubations.

In autumn, triplicate samples for the determination of the partial pressure of CO_2 (pCO_2) were collected in 60 ml plastic syringes directly from the Niskin. The pCO_2 was measured with an infra-red gas analyzer (Licor Li-840) after headspace equilibration in the syringe (Abril et al., 2015; Borges et al., 2015). The Li-840 was calibrated with N_2 and certified CO_2:N_2 mixtures (Air Liquide, Belgium) of 388, 813, 3788 and 8300 ppm CO_2. The precision of measurements was $\pm4.1\%$.

Water extracted for creating the headspace in the serum bottles was used to quantify SO_4^{2-}, NH_4^+, NO_2^-, NO_3^-, Mn and Fe concentrations. SO_4^{2-}, NO_2^- and NH_4^+ concentrations were quantified colorimetrically using a 5-cm optical path and a Genesys 10vis spectrophotometer (Thermo Spectronic). SO_4^{2-} concentrations were determined by the nephelometric method according to Rodier et al. (1996), after being precipitated in barium sulfate in an acid environment. NH_4^+ concentrations were determined using the dichloroisocyanurate-salicylate-nitroprussiate colorimetric method (Westwood, 1981), and NO_2^- concentrations were determined by the sulfanilamide coloration method (APHA, 1998). NO_3^- concentrations were determined after vanadium reduction to NO_2^- and quantified with a Multiskan Ascent Thermo Scientific multiplates reader (APHA, 1998; Miranda et al., 2001). The detection limits for these methods were 52, 0.3, 0.15 and 0.03 μmol L^{-1}, for SO_4^{2-}, NH_4^+, NO_3^- and NO_2^-, respectively.

The samples for total Fe and Mn determination were digested and mineralized in nitric acid, using specific Teflon bombs in a microwave digestion labstation (Ethos D, Milestone Inc.). They were finally diluted into milli-Q water to a volume of 50 ml. The total Fe and Mn concentrations were determined by inductively coupled plasma mass spectrometry (ICP-MS) using dynamic reaction cell (DRC) technology (ICP-MS SCIEX ELAN DRC II, PerkinElmer inc.). Analytical accuracy was verified by a certified reference material (BCR 715, Industrial Effluent Wastewater).

Additional samples to determine vertical profiles of NO_3^-, NH_4^+,

NO_2^-, PO_4^{3-} and SO_4^{2-} concentrations were collected in 50 ml plastic vials after being filtered through a 0.22 μm syringe filter, and stored frozen. NO_3^-, NO_2^-, NH_4^+ and SO_4^{2-} concentrations were determined according to respective methods described above. PO_4^{3-} concentrations were determined colorimetrically with a 5-cm optical path, in a spectrophotometer Thermo Spectronic Genesys 10vis, using the ammonium molybdate-potassium antimonyl tartrate method (APHA, 1998). The detection limit of this method was 0.03 μmol L^{-1}.

Samples to determine vertical profiles of H_2S concentrations were collected in 60 ml biological oxygen demand bottles after being filtered through a 0.22 μm syringe filter, and preserved with 2 ml of 1 mol L^{-1} zinc acetate. Concentrations were determined colorimetrically as described above, using the analytical method described by Cline (1969).

In summer and autumn, an additional 60 mL glass serum bottle per depth was collected and preserved as described above in order to measure the $\delta^{13}C$ values of CH_4 ($\delta^{13}C$-CH_4). $\delta^{13}C$-CH_4 was then determined by a custom developed technique (Morana et al., 2015), whereby a 5 ml helium headspace was first created and CH_4 was flushed out through a double-hole needle. CO_2 and H_2O were first removed with a CO_2 trap (soda lime) and a water trap (magnesium perchlorate) and then the non-methane volatile organic molecules were trapped and hence removed from the gas stream in a loop immerged in liquid nitrogen. The CH_4 was converted to CO_2 in an online combustion column similar to that in an Elemental Analyzer. The resulting CO_2 was subsequently preconcentrated by immersion of a stainless steel loop in liquid nitrogen passed through a micropacked GC column (HayeSep Q 2 m, 0.75 mm ID; Restek), and finally measured on a Thermo DeltaV Advantage isotope ratio mass spectrometer. CO_2 produced by acidification (H_3PO_4) of certified reference standards for $\delta^{13}C$ analysis (IAEA-CO1 and LSVEC) was used to calibrate $\delta^{13}C$-CH_4 data. Reproducibility estimated based on duplicate injection of a selection of samples was typically better than ±0.5‰.

2.3. CO_2, CH_4 and N_2O fluxes calculations

CO_2, CH_4 and N_2O fluxes to the atmosphere were calculated from the dissolved concentration at 1 m depth from which was computed the concentration gradient across the air-water interface of CO_2, CH_4 and N_2O, and the gas transfer velocity computed from wind speed according to the Cole and Caraco (1998) relationship. A positive flux value corresponds to a net gas transfer from the water to the atmosphere, while a negative flux corresponds to a net gas transfer from the atmosphere to the water. Wind speeds were obtained from the National Centers for Environmental Prediction (NCEP) gridded daily product (grid point: 50.4752°N, 3.7500°E).

3. Results

3.1. Physico-chemical parameters

The position of thermoclines and chemoclines (specific conductivity and pH) strongly differed between seasons (Fig. 1). The water column was well stratified during the sampling in spring, summer and autumn, with thermoclines located in the upper part of the water column (first 10 m), while in winter, the water column was mixed from surface to 20 m. Surface temperatures were higher in spring and summer (maximum 18 °C at 1 m depth), lowest in winter (5 °C at 1 m depth), and intermediate in autumn (14 °C at 1 m depth).

During winter, when the water column was almost entirely mixed, the oxycline was located at the bottom of the lake (20 m) (Fig. 1). However, the oxycline moved upward following the establishment of the thermal stratification in spring, to reach 7 m

and 8.5 m in summer and autumn, respectively. In spring, summer and winter, significant N_2O concentration peaks were observed, with a maximum of 440 nmol L^{-1} recorded at 14 m in summer. In autumn, the distribution of N_2O was more uniform than during the other seasons, with highest N_2O concentrations of 35 nmol L^{-1}. Except during winter when the peak was observed at the oxic-anoxic interface, N_2O peaks were observed below the oxycline, in anoxic waters during the other three seasons. The pCO_2 value in autumn (1560 ppm at 1 m depth) was well above the atmospheric equilibrium (390 ppm) in oxic surface waters and strongly increased in anoxic waters to reach ~18,000 ppm. The CH_4 concentrations strongly increased in anoxic waters (up to 618 μmol L^{-1}) but were also quite important in oxic waters, especially in winter (up to 30 μmol L^{-1} at 1 m depth), and ranged between 0.6 and 1 μmol L^{-1} at 1 m depth during the other three seasons. During summer, $\delta^{13}C$-CH_4 were stable in bottom waters (~−75‰) but started to gradually increase at 10 m, slightly below the base of the oxycline, to reach a maximum of −45‰ between 8.5 and 6 m. In autumn, similarly low $\delta^{13}C$-CH_4 (−75‰) were measured in bottom waters but the increase near the oxic-anoxic interface was more abrupt.

Vertical profiles of NO_3^- and NO_2^- strongly differed between seasons (Fig. 1). Important NO_3^- accumulation zones (nitraclines) were observed in both oxic and anoxic waters in spring and at the oxic-anoxic interface in summer. The maximum NO_3^- concentration was 70 and 30 μmol L^{-1} in spring and summer, respectively. In autumn and winter, no nitracline was observed, but instead NO_3^- concentrations were quite stable throughout the oxic part of the water column (around 15 and 20 μmol L^{-1} in autumn and winter, respectively), and decreased down to 1 μmol L^{-1} in anoxic waters. Except in autumn where NO_2^- concentrations remained low (below 1 μmol L^{-1}) throughout the water column, important NO_2^- concentrations peaks were also observed. In spring and summer, the maximum peaks of 10 and 20 μmol L^{-1}, respectively, were located in anoxic waters. In winter, maximum peak was slightly lower (8 μmol L^{-1}) and was located at the oxic-anoxic interface. For each season, deep anoxic waters were rich in NH_4^+ and PO_4^{3-} (up to 190 and 22 μmol L^{-1}, respectively), while oxic waters were depleted in these nutrients. However, higher concentrations were observed in oxic waters in winter than in other seasons. Indeed NH_4^+ and PO_4^{3-} concentrations were around 35 and 2 μmol L^{-1}, respectively, all along the oxic part of the water column in winter, while NH_4^+ concentrations were below 5 μmol L^{-1} and PO_4^{3-} concentrations below detection in other seasons.

For each season, total Fe and Mn concentrations were quite high in anoxic waters. The maximum Fe concentration peak of 23 μmol L^{-1} was observed in summer, while the maximum Mn concentration peak of 15 μmol L^{-1} was observed in autumn. SO_4^{2-} concentrations were high all along the vertical profiles (ranging between 354 and 1537 μmol L^{-1}), but tended to decrease in deep anoxic waters, co-occurring with an increase of H_2S concentrations (Fig. 1).

3.2. CH_4 oxidation

CH_4 oxidation was observed during all seasons (Fig. 2). In spring, important rates were observed in both oxic and anoxic waters, without Mo added, up to 4 and 3 μmol L^{-1} d^{-1}, respectively. In summer, no CH_4 oxidation was observed in oxic waters. However, important CH_4 oxidation rates were observed in anoxic waters, without and with Mo added. Without Mo added, the two maximum peaks of 9 and 6 μmol L^{-1} d^{-1} were observed at 14 and 18 m depth, respectively. These peaks co-occurred with important NO_3^- and SO_4^{2-} consumption peaks, up to 2 and 20 μmol L^{-1} d^{-1}, respectively. A NO_2^- consumption peak of 0.4 μmol L^{-1} d^{-1} was also observed at
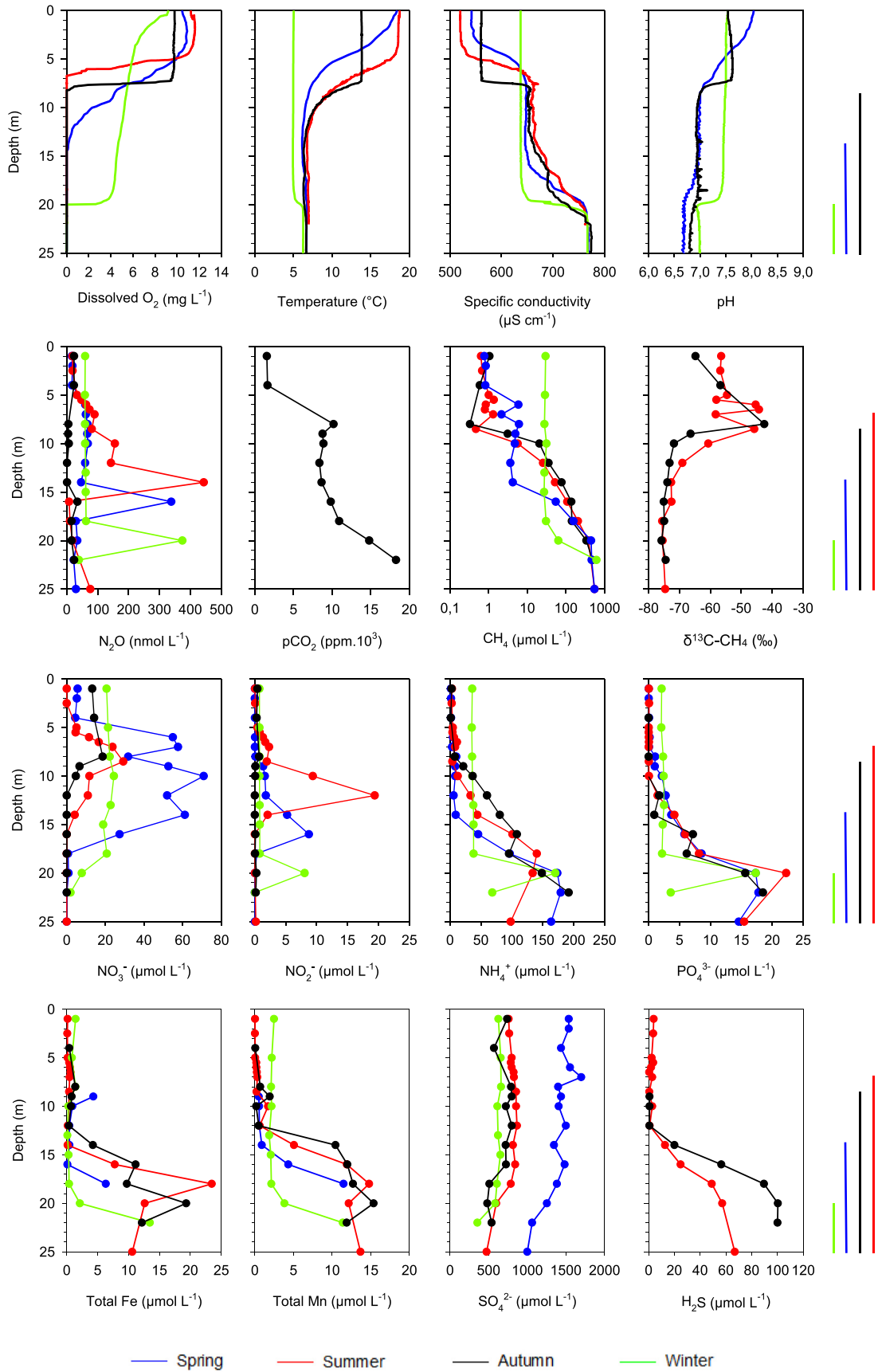
Fig. 1. Vertical profiles of dissolved oxygen (mg L^{-1}), temperature (°C), specific conductivity (μS cm^{-1}), pH, N$_2$O concentrations (nmol L^{-1}), pCO$_2$ (ppm.10^3), CH$_4$ concentrations (μmol L^{-1}), δ^{13}C-CH$_4$ (‰), nutrients (NO$_3^-$, NO$_2^-$, NH$_4^+$, PO$_4^{3-}$), total Fe, total Mn, SO$_4^{2-}$ and H$_2$S concentrations (μmol L^{-1}) in spring (blue), summer (red), autumn (black) and winter (green). Vertical lines to the right represent the anoxic layer for each season (same color code). Note the X log scale for CH$_4$ concentrations. (For interpretation of the references to colour in this figure legend, the reader is referred to the web version of this article.)

14 m, and another one was also observed in oxic waters. With Mo added, oxidation peaks were observed at the same depths, but rates were lower than without Mo. Important NO_3^- consumption peaks were also observed at 14 and 18 m, up to 5.5 μmol L^{-1} d^{-1}, so higher than without Mo added.

In autumn, important oxidation rates were measured throughout the anoxic zone, while no CH_4 oxidation was observed in oxic waters. The maximum oxidation rate of ~15 μmol L^{-1} d^{-1} was observed at 20 m, with and without Mo added. Except at 20 m where CH_4 oxidation rate with Mo was slightly higher than without Mo, CH_4 oxidation rates were always lower with Mo added. Without Mo added, only one peak of NO_3^- consumption was observed, at 10 m, and thus co-occurred with the first oxidation peak. One SO_4^{2-} consumption peak of 14 μmol L^{-1} d^{-1} was observed at 12 m. Below 14 m, SO_4^{2-} consumption linearly increased. No measurable NO_2^- consumption was observed. With Mo added, NO_3^- consumption was observed just below the oxic-anoxic interface and linearly decreased in anoxic waters, following the same pattern than CH_4 oxidation until 12 m depth. In winter, an aerobic oxidation rate of 1 μmol L^{-1} d^{-1} was observed at 18 m. Without Mo added, the maximum oxidation peak of 4 μmol L^{-1} d^{-1} was observed at the oxic-anoxic interface, and no oxidation was observed below 20 m. A NO_3^- consumption rate of 3 μmol L^{-1} d^{-1} was observed at the same depth, and SO_4^{2-} consumption strongly increased below 20 m (until 37 μmol L^{-1} d^{-1}). No NO_2^- consumption was observed. With Mo added, no aerobic CH_4 oxidation was observed. Also, the CH_4 oxidation peak observed at 20 m was slightly higher (5 μmol L^{-1} d^{-1}) and an oxidation peak of 6 μmol L^{-1} d^{-1} was observed at 22 m depth. NO_3^- consumption was lower than without Mo at 20 m depth, but was higher at 22 m.

3.3. CH_4, N_2O and CO_2 fluxes

CH_4 and N_2O air-water fluxes were estimated during the four seasons, and CO_2 air-water flux was estimated for autumn (Table 1). The maximum CH_4 flux of 12,482 μmol m^{-2} d^{-1} was observed in winter, while CH_4 fluxes were similar in spring, summer and autumn (mean of 641 μmol m^{-2} d^{-1}). N_2O fluxes were quite constant all along the year (mean of 17 μmol m^{-2} d^{-1} for summer, autumn and winter), except in spring where the flux was distinctly lower (5 μmol m^{-2} d^{-1}). The CO_2 flux in autumn was 67,000 μmol m^{-2} d^{-1}.

4. Discussion

Physico-chemical parameters (temperature, specific conductivity, pH and oxygen) showed that the mixed layer depth varied according to the season, but that the deepest part of the water column (below 20 m) was anoxic throughout the year. Oxygen concentrations in surface waters were also higher in summer and spring, which can be linked with higher temperatures and irradiance favoring phytoplankton activity, and oxygen production through photosynthesis.

Higher water temperatures also enhance bacterial activity, and denitrification and nitrification, which both produce N_2O, are known to be enhanced when temperature increases (Saad and Conrad, 1993; Van Hulle et al., 2010; Dong et al., 2011). High N_2O concentrations were observed in summer and spring. In spring, the maximum N_2O peak was located at 16 m, and co-occurred with the maxima in NO_2^- concentration and NO_3^- consumption rate. In summer, the maximum N_2O peak was observed at 14 m depth, and also co-occurred with the maximum NO_3^- consumption rate. Altogether, these observations reflect the occurrence of denitrification in the anoxic water of the lake. Heterotrophic denitrification requires organic matter and NO_3^- supply. The higher NO_3^-

concentrations were observed in spring, when nitrification is favored by higher temperatures and abundant NH_4^+ following winter-time mixing.

Denitrification can be heterotrophic, with organic matter as electron donor, but can also be autotrophic with other electron donors. One of these electron donors can be CH_4. AOM coupled with NO_3^- reduction (NDMO) is still poorly understood. However, it is thermodynamically highly favorable (Borrel et al., 2011) and can thus be of great importance in anoxic environments with high NO_3^- concentrations. During this study, we investigated CH_4 oxidation using two different approaches. The first one was the measurement of the $\delta^{13}C$ of dissolved CH_4 along the depth profile in summer and autumn. While $\delta^{13}C$-CH_4 values in deep waters were very low (~65‰), significant increases of $\delta^{13}C$-CH_4 values were observed between 6 and 8.5 m depth in summer (at the oxic-anoxic interface and in anoxic waters, until −44‰), and at 8 m depth in autumn (also at the oxic-anoxic interface, until −43‰). During microbial processes, isotopic fractionation occurs, since organisms preferentially use the lighter isotopes. Therefore, during CH_4 oxidation, bacteria preferentially use ^{12}C-CH_4 and the residual CH_4 pool is then enriched in ^{13}C. For both seasons, the increases of $\delta^{13}C$-CH_4 values co-occurred with a strong decrease of CH_4 concentrations, at the oxic-anoxic interfaces. Hence, the vertical profiles of $\delta^{13}C$-CH_4 strongly suggest that a large part of CH_4 was oxidized within a 5 m depth interval, in summer and autumn. In autumn, it also co-occurred with a strong increase in pCO_2. In autumn and summer, $\delta^{13}C$-CH_4 decreased from the base of the oxic layer towards surface waters, by ~22 and ~12‰, respectively. Such a decrease cannot be related to exchange with the atmosphere since the atmospheric $\delta^{13}C$-CH_4 is close to −47‰ (Quay et al., 1999). A possible explanation would be CH_4 production in oxic conditions related to primary production by pathways that remain elusive (Tang et al., 2016) as recently reported in several lakes (Grossart et al., 2011; Bogard et al., 2014; Tang et al., 2014). Such an explanation is consistent with the eutrophic nature of the Dendre Lake and should be further investigated in future.

The fraction of the CH_4 flux oxidized in a given depth interval was calculated according to the following equation (Coleman et al., 1981):

$$\ln(1-f) = \ln((\delta^{13}C\text{-}CH_{4t} + 1000)/(\delta^{13}C\text{-}CH_{4b} + 1000))/((1/\alpha)-1)$$

where f is the fraction of CH_4 oxidized in the depth interval, $\delta^{13}C$-CH_{4t} and $\delta^{13}C$-CH_{4b} are the $\delta^{13}C$-CH_4 values at the top and at the bottom of the depth interval, respectively, and α is the isotope fractionation factor.

Coleman et al. (1981) showed that α was dependent on temperature. Bastviken et al. (2002) determined a α of 1.0196 $\pm$ 0.002 for three Swedish lakes, whose temperature profiles are closer to what we observed. Based on this approach, we computed that in the Dendre Lake in summer, a large fraction (70–73%) of the upward flux of CH_4 was oxidized in a narrow depth interval (between 8.5 and 12 m; anoxic waters). The same observation is made in autumn, since 81–83% was oxidized between 8 and 10 m depth (mostly in anoxic waters). This isotopic approach clearly shows the importance of the AOM in the water column of the pit stone lake of the Dendre.

In addition to these indirect estimations of CH_4 oxidation, we directly quantified CH_4 oxidation in incubation experiments during which the evolution of CH_4 concentrations was measured through time. Our incubations focused on AOM and fewer measurements were made in oxic waters. In spring, quite important aerobic CH_4 oxidation rates were observed. If we integrate aerobic rates over the oxic water column (from 0 to 13 m), we obtain an estimated aerobic oxidation rate of 38 μmol m^{-2} d^{-1}. If we do the same for the anoxic
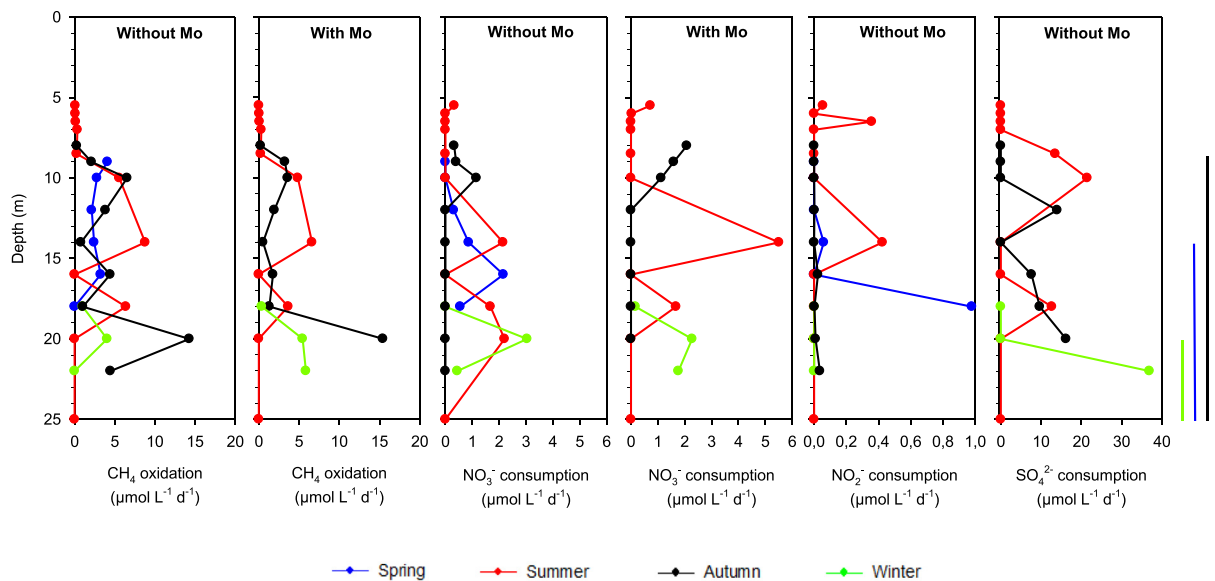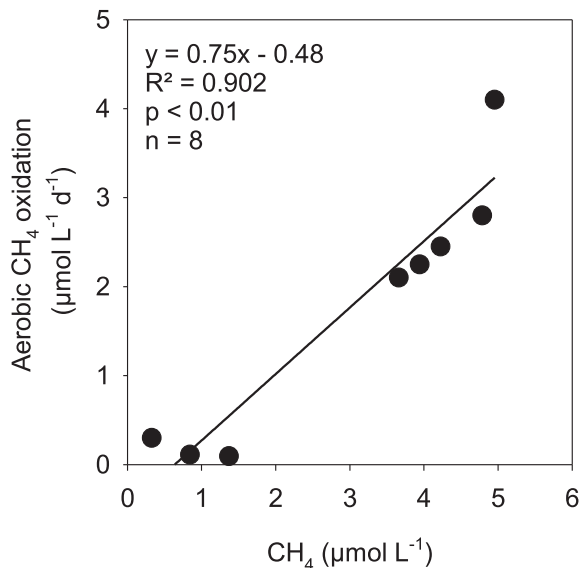
Fig. 2. Vertical profiles of CH_4 oxidation rates (μmol L^{-1} d^{-1}) without and with molybdate (Mo) added, NO_3^- consumption rates (μmol L^{-1} d^{-1}) without and with Mo added, NO_2^- and SO_4^{2-} consumption rates (μmol L^{-1} d^{-1}) without Mo added, in spring (blue), summer (red), autumn (black) and winter (green). Vertical lines to the right represent the anoxic layer for each season (same color code). (For interpretation of the references to colour in this figure legend, the reader is referred to the web version of this article.)

Table 1
CH_4, N_2O and CO_2 fluxes (μmol m^{-2} d^{-1}) to the atmosphere during the different seasons. Nd: not determined.

	CH_4 fluxes	N_2O fluxes	CO_2 fluxes
Spring	633	5	Nd
Summer	1000	18	Nd
Autumn	564	13	67,000
Winter	12,482	19	Nd

Fig. 3. CH_4 concentrations (μmol L^{-1}) in oxic waters compared with aerobic CH_4 oxidation rates (μmol L^{-1} d^{-1}), for all seasons.

water column (from 14 to 25 m), only 10 μmol m^{-2} d^{-1} were anaerobically oxidized. These estimates suggest that aerobic CH_4 oxidation was the main pathway of CH_4 oxidation in spring, yet AOM still accounted for 21% of total CH_4 oxidation (Table 2). In summer, three measurements of aerobic CH_4 oxidation were also made at 5.5, 6 and 6.5 m depth. Very low CH_4 oxidation rates were observed (mean of 0.2 μmol L^{-1} d^{-1}) in oxic waters, while the maximum AOM rate was estimated to 9 μmol L^{-1} d^{-1} at 14 m, in accordance with $\delta^{13}C$-CH_4 data. In summer, AOM was clearly the main pathway of CH_4 oxidation, accounting for 99% of total CH_4 oxidation (Table 2). As shown in Fig. 3, aerobic CH_4 oxidation highly depends on CH_4 concentrations, confirming a strong substrate control of CH_4 oxidation (e.g. Guérin and Abril, 2007). CH_4 concentrations in oxic waters were higher in spring than in summer, with means of 5 and 1 μmol L^{-1} at depths where oxidation was measured, respectively. These important differences may be explained by the mixed layer depth of the water column. In spring, the water column was anoxic deeper, so CH_4 produced in anoxic waters was anaerobically oxidized over a less important depth than in summer, where the water was anoxic at 7 m. Moreover, higher

water temperatures observed in summer might enhance CH_4 oxidation. In spring, a greater amount of CH_4 could thus reach the oxic waters, explaining higher CH_4 concentrations observed, and so higher aerobic CH_4 oxidation rates. Fig. 4a shows the dependence of depth-integrated oxidation rates with the depth of the oxygenated

Table 2
Depth-integrated CH_4 oxidation rates (μmol m^{-2} d^{-1}) through all the water column, and percentages of aerobic and anaerobic CH_4 oxidation, for the four seasons.

|	Depth-integrated oxidation rates (μmol m^{-2} d^{-1})	Aerobic oxidation (%)	Anaerobic oxidation (%)
Spring	48	79	21
Summer	67	1	99
Autumn	70	3	97
Winter	27	77	23

layer. Depth-integrated oxidation rates were lower when the oxy-cline was located deeper, so in winter and spring, which shows the importance of the anaerobic compartment. Also, as shown by Fig. 4b, higher CH_4 oxidation rates correspond to lower CH_4 fluxes, illustrating the importance of CH_4 oxidation to prevent CH_4 emissions to the atmosphere. In correlation with Fig. 4a and b, Fig. 4c shows that a deeper oxycline is linked to higher CH_4 fluxes.

Incubations also revealed important AOM rates. Because NO_3^- and SO_4^{2-} concentrations in the water column were high, we also measured the evolution of these concentrations in the incubations,
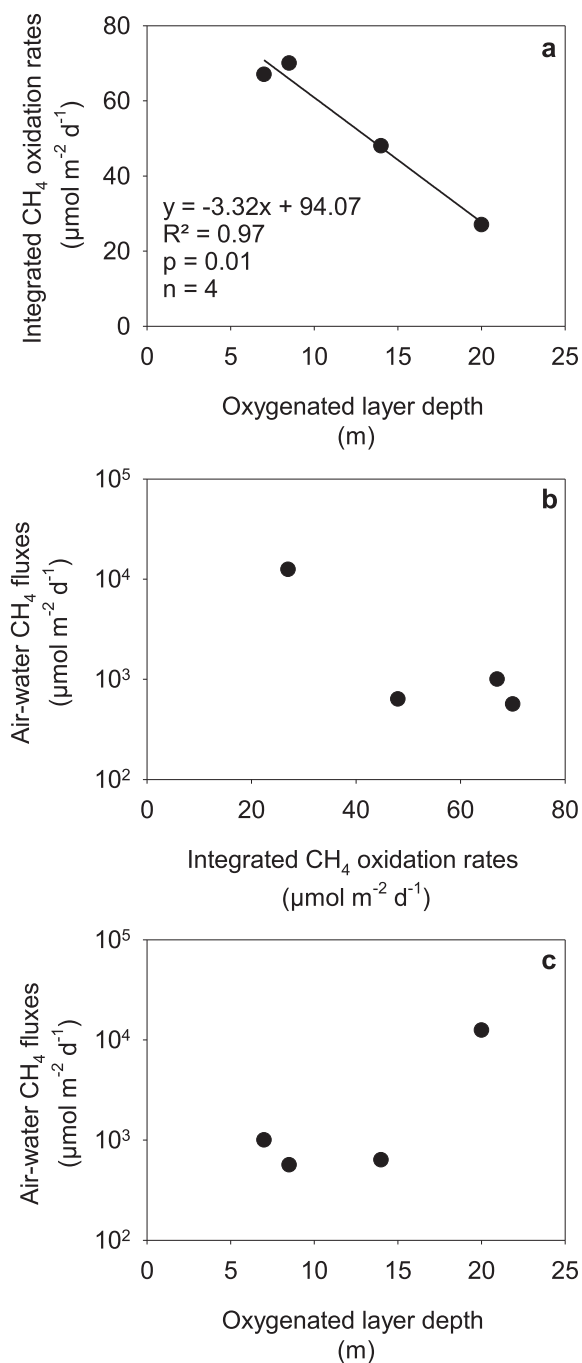
Fig. 4. (**a**) Depth-integrated CH_4 oxidation rates ($\mu mol\ m^{-2}\ d^{-1}$) compared with depth of the oxygenated layer (m) and air-water CH_4 fluxes ($\mu mol\ m^{-2}\ d^{-1}$) compared with (**b**) depth-integrated CH_4 oxidation rates ($\mu mol\ m^{-2}\ d^{-1}$) and (**c**) depth of the oxygenated layer (m), for all seasons. Note the Y log scales for b and c.

in order to determine if these elements might be AOM electron acceptors. In spring, summer and winter, all the AOM peaks co-occurred with NO_3^- consumption peaks. In autumn, only the first AOM peak observed at 10 m depth co-occurred with the peak of NO_3^- consumption. These results strongly suggest the existence of a coupling between CH_4 oxidation and NO_3^- reduction. However, the observed NO_3^- consumption rates are not sufficient to be responsible for the observed AOM rates (Fig. 5a). These calculations are based on stoichiometry of the following equation, according to which 8 mol of NO_3^- are needed for the oxidation of 5 mol of CH_4 (Raghoebarsing et al., 2006):

$$5CH_4 + 8NO_3^- + 8H^+ \rightarrow 5CO_2 + 4N_2 + 14H_2O \tag{1}$$
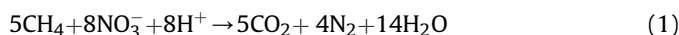
The other electron acceptor present at high concentrations is SO_4^{2-}. SO_4^{2-} concentrations were high throughout all vertical profiles, and tended to decrease in anoxic waters, when H_2S concentrations increased, showing a SO_4^{2-} reduction zone. In our incubations, we observed important SO_4^{2-} consumption rates that can potentially contribute to the AOM. Indeed, SO_4^{2-} consumption rates are sufficient to explain AOM rates observed at some depths. Moreover, when we inhibited sulfate-reducing bacteria by the addition of Mo, we tended to observe lower AOM rates, strongly suggesting a coupling between AOM and SO_4^{2-} reduction. However, AOM was not fully inhibited, and we can invoke two different reasons to explain this. First, the specific inhibitor used (molybdate) may not be fully efficient, as suggested by Nauhaus et al. (2005) who demonstrated that the two distinct archaeal communities capable of AOM (ANME-I and ANME-II) reacted differently to molybdate, with an incomplete inhibition of ANME-I for the same concentrations of inhibitor. Because we did not perform pyrose-quencing analyses in our study, we cannot determine relative community dominance. A second mechanism to explain why AOM was not fully inhibited when molybdate was added, is that SDMO is not the only AOM pathway in the water column of the Dendre stone pit lake, confirming the potential occurrence of NDMO, as described above.

We must note that AOM rates calculated on the basis of NO_3^- and SO_4^{2-} consumption rates are potential maximum rates, since we consider here that NO_3^- and SO_4^{2-} reduction occurs only with CH_4 as electron donor, which is unlikely. Heterotrophic denitrification and SO_4^{2-} reduction with organic matter are both more favorable, especially in an environment with high organic matter supply.

We can thus hypothesize that AOM occurred with different electron acceptors in the Dendre stone pit lake. As NDMO is thermodynamically more favorable than SDMO, and as NO_3^- concentrations are relatively high, we suppose that AOM firstly occurs with NO_3^- as electron acceptor. When NO_3^- becomes depleted, AOM can occur with SO_4^{2-}, since SDMO is less favorable but SO_4^{2-} concentrations are higher than NO_3^- concentrations. Fig. 5b shows CH_4 oxidation rates calculated on the basis of SO_4^{2-} consumption rates (according to stoichiometry of equation (2); Borrel et al., 2011) compared with measured CH_4 oxidation rates.

$$CH_4 + SO_4^{2-} \rightarrow HCO_3^- + HS^- + H_2O \tag{2}$$
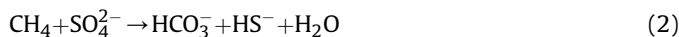
This shows that most of the AOM must be coupled with SO_4^{2-} reduction (data points to the right side of the 1:1 line in Fig. 5b), but that SO_4^{2-} is not the only electron acceptor, since some oxidation rates cannot be explained by SO_4^{2-} consumption rates alone (data points to the left side of the 1:1 line in Fig. 5b). We must note that calculated AOM rates associated with SO_4^{2-} are higher than measured AOM rates, illustrating that not all the SO_4^{2-} consumption is linked to CH_4 oxidation. Also, calculated AOM rates based on NO_3^- and SO_4^{2-} consumption rates are potential maximum rates, since in
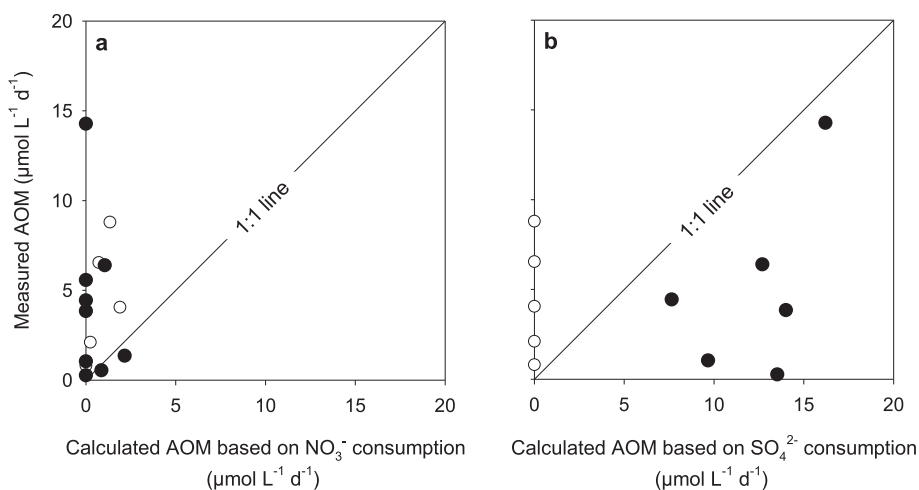
Fig. 5. Measured AOM (μmol L^{-1} d^{-1}) compared with AOM calculated on base on (a) NO$_3^-$ and (b) SO$_4^{2-}$ consumption rates (μmol L^{-1} d^{-1}), for all seasons. White dots are AOM rates measured with no observation of SO$_4^{2-}$ consumption.

our calculations, we consider that all NO$_3^-$ and SO$_4^{2-}$ reduction occurs only with CH$_4$ as electron donor. In any case, NO$_3^-$ can thus be responsible for a part of the AOM not explained by SO$_4^{2-}$ (at the left of the 1:1 line) but it is not sufficient, which means that other electron acceptors must be involved, such as Fe and Mn. Total Fe and Mn concentrations were relatively high in the water column and can thus potentially contribute to AOM. In summer and autumn in particular, higher Fe and Mn concentration peaks co-occurred with high CH$_4$ oxidation peaks.

Regardless of the electron acceptors, AOM rates in the Dendre stone pit lake were quite high compared to other temperate or boreal lakes reported in literature (Table 3) and must thus contribute to limited atmospheric CH$_4$ fluxes. CH$_4$ concentrations in oxic waters were also high. In winter, in particular, CH$_4$ concentrations in oxic waters were up to 30 μmol L^{-1}, which can be linked to the mixing of the water column. The annual average of CH$_4$ concentrations in surface waters was 8.1 μmol L^{-1} which is one order of magnitude higher than the global average of lakes of the same size class (0.01–0.1 km^2) of 0.7 μmol L^{-1} reported by Holgerson and Raymond (2016). The corresponding median of CH$_4$ emission to the atmosphere (816 μmol m^{-2} d^{-1}) in the Dendre Lake is also high compared to other lakes globally, since the global median of diffusive CH$_4$ fluxes from lakes at the same latitude reported by Bastviken et al. (2011) is 263 μmol m^{-2} d^{-1}, while the global flux for lakes of the same size class reported by Holgerson and Raymond (2016) is 279 μmol m^{-2} d^{-1}.

Bastviken et al. (2011) also reported fluxes due to the emission of CH$_4$ stored in the water column during lake overturn. The median value of these fluxes plus the diffusive fluxes is estimated to

1000 μmol m^{-2} d^{-1} (Bastviken et al., 2011) that is lower than CH$_4$ emissions estimated in the Dendre stone pit lake in winter (12,482 μmol m^{-2} d^{-1}). So high CH$_4$ fluxes in winter in the Dendre stone pit lake can be explained by an accumulation of CH$_4$ in anoxic waters during the stratification periods, which are mixed with the oxic waters during lake overturn, as described above. As water temperatures are low, microbial CH$_4$ oxidation in winter is reduced and does not consume the high stock of CH$_4$, which can escape to the atmosphere. High CH$_4$ production in the water column of the Dendre Lake can be explained by a high primary production due to high nutrient availability. Indeed, high DIN (57 μmol L^{-1}) and PO$_4^{2-}$ (2 μmol L^{-1}) concentrations observed in surface waters (at 5 m) illustrate the eutrophic status of the lake. This is not surprising considering that this stone pit lake is mainly fed by ground waters, which are enriched in DIN from extensive fertilizer use on cropland (SPW-DGO3, 2015).

The N$_2$O fluxes were higher in summer, autumn and winter, with a mean of 17 μmol m^{-2} d^{-1}. In spring, N$_2$O flux was estimated to 5 μmol m^{-2} d^{-1}. Lower N$_2$O flux, linked to lower N$_2$O concentrations in surface waters observed in spring, might be linked to higher bacterial activity and therefore more efficient denitrification, leading to a stronger N$_2$O consumption. Compared with fluxes reported by Huttunen et al. (2003) for five boreal lakes, N$_2$O fluxes measured in the Dendre stone pit lake were very high, and no negative flux was observed, suggesting that the water column was a source of N$_2$O for the atmosphere all the year. These higher N$_2$O emissions can also be related to high DIN concentrations.

In conclusion, this study demonstrates the occurrence of AOM in the water column of a small freshwater body. Results show that AOM occurred with SO$_4^{2-}$ as electron acceptor, but also strongly suggest that AOM also occurred with NO$_3^-$ reduction. Further studies are nevertheless needed to clearly identify these processes, such as incubations spiked with the addition of the different potential electron acceptors for AOM and description of the microbial community composition. In this study, we also demonstrate that a flooded quarry can be a significant source of atmospheric greenhouse gases. While the majority of eutrophic agriculturally impacted lakes are net CO$_2$ sinks (Balmer and Downing, 2011), we suggest that these systems can be extreme emitters of other potent greenhouse gases such as CH$_4$ and N$_2$O, in response to nitrogen enrichment and high primary productivity.

Table 3
Anaerobic CH$_4$ oxidation rates (μmol L^{-1} d^{-1}) from other lakes in literature.

Lake	AOM rate	Source
Dendre	Seasonal means: 2 – 5 Maximum: 15	**This study**
Marn (Sweden)	2.2	Bastviken et al. (2002)
Illersjoen (Sweden)	1.3–3.0	Bastviken et al. (2002)
Pavin (France)	0.4	Lopes et al. (2011)
Mendota (US)	5.8	Harrits and Hanson (1980)
Big Soda (US)	0.06	Iversen et al. (1987)
Mono (US)	0.08	Oremland et al. (1993)
Tanganyika (Africa)	0.24–1.8	Rudd et al. (1974)

Acknowledgements

References

á Norði, K., Thamdrup, B., 2014. Nitrate-dependent anaerobic methane oxidation in a freshwater sediment. Geochim. Cosmochim. Acta 132, 141–150.

á Norði, K., Thamdrup, B., Schubert, C.J., 2013. Anaerobic oxidation of methane in an iron- rich Danish freshwater lake sediment. Limnol. Oceanogr. 58, 546–554.

Abril, G., Bouillon, S., Darchambeau, F., Teodoru, C.R., Marwick, T.R., Tamooh, F., Ochieng Omengo, F., Geeraert, N., Deirmendjian, L., Polsenaere, P., 2015. Technical Note: large overestimation of pCO2 calculated from pH and alkalinity in acidic, organic-rich freshwaters. Biogeosciences 12, 67–78.

APHA, 1998. Standard Methods for the Examination of Water and Wastewater. Washington.

Balmer, M.B., Downing, J.A., 2011. Carbon dioxide concentrations in eutrophic lakes: undersaturation implies atmospheric uptake. Inland Waters 1, 125–132.

Bastviken, D., Ejlertsson, J., Tranvik, L., 2002. Measurement of methane oxidation in lakes: a comparison of methods. Environ. Sci. Technol. 36, 3354–3361.

Bastviken, D., Tranvik, L.J., Downing, J.A., Crill, P.M., Enrich-Prast, A., 2011. Freshwater methane emissions offset the continental carbon sink. Science 331, 50.

Boetius, A., Ravenschlag, K., Schubert, C.J., Rickert, D., Widdel, F., Gieseke, A., Amann, R., Jørgensen, B.B., Witte, U., Pfannkuche, O., 2000. A marine microbial consortium apparently mediating anaerobic oxidation of methane. Nature 407, 623–626.

Bogard, M.J., del Giorgio, P.A., Boutet, L., Chaves, M.C.G., Prairie, Y.T., Merante, A., Derry, A.M., 2014. Oxic water column methanogenesis as a major component of aquatic CH4 fluxes. Nat. Commun. 5.

Borges, A.V., Darchambeau, F., Teodoru, C.R., Marwick, T.R., Tamooh, F., Geeraert, N., Omengo, F.O., Guérin, F., Lambert, T., Morana, C., 2015. Globally significant greenhouse-gas emissions from African inland waters. Nat. Geosci. 8, 637–642.

Borrel, G., Jézéquel, D., Biderre-Petit, C., Morel-Desrosiers, N., Morel, J.-P., Peyret, P., Fonty, G., Lehours, A.-C., 2011. Production and consumption of methane in freshwater lake ecosystems. Res. Microbiol. 162, 832–847.

Cline, J.D., 1969. Spectrophotometric determination of hydrogen sulfide in natural waters. Limnol. Oceanogr. 14, 454–458.

Cole, J.J., Caraco, N.F., 1998. Atmospheric exchange of carbon dioxide in a low-wind oligotrophic lake measured by the addition of SF6. Limnol. Oceanogr. 43, 647–656.

Coleman, D.D., Risatti, J.B., Schoell, M., 1981. Fractionation of carbon and hydrogen isotopes by methane-oxidizing bacteria. Geochim. Cosmochim. Acta 45, 1033–1037.

Crowe, S., Katsev, S., Leslie, K., Sturm, A., Magen, C., Nomosatryo, S., Pack, M., Kessler, J., Reeburgh, W., Roberts, J., 2011. The methane cycle in ferruginous Lake Matano. Geobiology 9, 61–78.

Deutzmann, J.S., Schink, B., 2011. Anaerobic oxidation of methane in sediments of Lake Constance, an oligotrophic freshwater lake. Appl. Environ. Microbiol. 77, 4429–4436.

Dong, L.F., Sobey, M.N., Smith, C., Rusmana, I., Phillips, W., Stott, A., Osborn, A.M., Nedwell, D.B., 2011. Dissimilatory reduction of nitrate to ammonium (DNRA) not denitrification or anammox dominates benthic nitrate reduction in tropical estuaries. Limnol. Oceanogr. 279–291.

Ettwig, K.F., Butler, M.K., Le Paslier, D., Pelletier, E., Mangenot, S., Kuypers, M.M., Schreiber, F., Dutilh, B.E., Zedelius, J., De Beer, D., 2010. Nitrite-driven anaerobic methane oxidation by oxygenic bacteria. Nature 464, 543–548.

Grossart, H.-P., Frindte, K., Dziallas, C., Eckert, W., Tang, K.W., 2011. Microbial methane production in oxygenated water column of an oligotrophic lake. PNAS 108, 19657–19661.

Guérin, F., Abril, G., 2007. Significance of pelagic aerobic methane oxidation in the methane and carbon budget of a tropical reservoir. J. Geophys. Res. Biogeosci. 112.

Haroon, M.F., Hu, S., Shi, Y., Imelfort, M., Keller, J., Hugenholtz, P., Yuan, Z., Tyson, G.W., 2013. Anaerobic oxidation of methane coupled to nitrate reduction in a novel archaeal lineage. Nature 500, 567–570.

Harrits, S.M., Hanson, R.S., 1980. Stratification of aerobic methane-oxidizing organisms in lake Mendota, Madison. Wis. Limnol. Oceanogr. 25, 412–421.

Holgerson, M.A., Raymond, P.A., 2016. Large contribution to inland water CO2 and CH4 emissions from very small ponds. Nat. Geosci. 9, 222–226.

Hu, S., Zeng, R.J., Keller, J., Lant, P.A., Yuan, Z., 2011. Effect of nitrate and nitrite on the selection of microorganisms in the denitrifying anaerobic methane oxidation process. Environ. Microbiol. Rep. 3, 315–319.

Huttunen, J.T., Alm, J., Liikanen, A., Juutinen, S., Larmola, T., Hammar, T., Silvola, J., Martikainen, P.J., 2003. Fluxes of methane, carbon dioxide and nitrous oxide in boreal lakes and potential anthropogenic effects on the aquatic greenhouse gas emissions. Chemosphere 52, 609–621.

IPCC, 2013. Climate Change 2013: the Physical Science Basis. Contribution of Working Group I to the Fifth Assessment Report of the Intergovernmental Panel on Climate Change. Cambridge University Press, Cambridge, United Kingdom and New York, NY, USA.

Iversen, N., Jørgensen, B., 1985. Anaerobic methane oxidation rates at the sulfate-methane transition in marine sediments from Kattegat and Skagerrak (Denmark). Limnol. Oceanogr. 30, 944–955.

Iversen, N., Oremland, R.S., Klug, M.J., 1987. Big Soda Lake (Nevada). 3. Pelagic methanogenesis and anaerobic methane oxidation. Limnol. Oceanogr. 32, 804–814.

Jones, R.I., Grey, J., 2011. Biogenic methane in freshwater food webs. Freshw. Biol. 56, 213–229.

Jørgensen, B.B., Weber, A., Zopfi, J., 2001. Sulfate reduction and anaerobic methane oxidation in Black Sea sediments. Deep-Sea Res. Pt. I 48, 2097–2120.

Kirschke, S., Bousquet, P., Ciais, P., Saunois, M., Canadell, J.G., Dlugokencky, E.J., Bergamaschi, P., Bergmann, D., Blake, D.R., Bruhwiler, L., Cameron-Smith, P., Castaldi, S., Chevallier, F., Feng, L., Fraser, A., Heimann, M., Hodson, E.L., Houweling, S., Josse, B., Fraser, P.J., Krummel, P.B., Lamarque, J.-F., Langenfelds, R.L., Le Quere, C., Naik, V., O'Doherty, S., Palmer, P.I., Pison, I., Plummer, D., Poulter, B., Prinn, R.G., Rigby, M., Ringeval, B., Santini, M., Schmidt, M., Shindell, D.T., Simpson, I.J., Spahni, R., Steele, L.P., Strode, S.A., Sudo, K., Szopa, S., van der Werf, G.R., Voulgarakis, A., van Weele, M., Weiss, R.F., Williams, J.E., Zeng, G., 2013. Three decades of global methane sources and sinks. Nat. Geosci. 6, 813–823.

Lopes, F., Viollier, E., Thiam, A., Michard, G., Abril, G., Groleau, A., Prévot, F., Carrias, J.-F., Albéric, P., Jézéquel, D., 2011. Biogeochemical modelling of anaerobic vs. aerobic methane oxidation in a meromictic crater lake (Lake Pavin, France). Appl. Geochem 26, 1919–1932.

Miranda, K.M., Espey, M.G., Wink, D.A., 2001. A rapid, simple spectrophotometric method for simultaneous detection of nitrate and nitrite. Nitric Oxide-Biol. Ch 5, 62–71.

Morana, C., Borges, A.V., Roland, F.A.E., Darchambeau, F., Descy, J.P., Bouillon, S., 2015. Methanotrophy within the water column of a large meromictic tropical lake (Lake Kivu, East Africa). Biogeosciences 12, 2077–2088.

Nauhaus, K., Treude, T., Boetius, A., Krüger, M., 2005. Environmental regulation of the anaerobic oxidation of methane: a comparison of ANME-I and ANME-II communities. Environ. Microbiol. 7, 98–106.

NOAA, 2015. The NOAA Annual Greenhouse Gas Index (AGGI). NOAA Earth System Research Laboratory, Broadway.

Oremland, R.S., Miller, L.G., Colbertson, C.W., Robinson, S., Smith, R.L., Lovley, D., Whiticar, M.J., King, G.M., Kiene, R.P., Iversen, N., 1993. Aspects of the Biogeochemistry of Methane in Mono Lake and the Mono Basin of California. Biogeochemistry of Global Change. Springer, pp. 704–741.

Quay, P., Stutsman, J., Wilbur, D., Snover, A., Dlugokencky, E., Brown, T., 1999. The isotopic composition of atmospheric methane. Glob. Biogeochem. Cy. 13, 445–461.

Raghoebarsing, A.A., Pol, A., Van de Pas-Schoonen, K.T., Smolders, A.J., Ettwig, K.F., Rijpstra, W.I.C., Schouten, S., Damsté, J.S.S., den Camp, H.J.O., Jetten, M.S., 2006. A microbial consortium couples anaerobic methane oxidation to denitrification. Nature 440, 918–921.

Rodier, J., Bazin, C., Broutin, J., Chambon, P., Champsaur, H., Rodi, L., 1996. L'Analyse de l'Eau (8ème édn). Dunod, Paris: France.

Rudd, J.W.M., Hamilton, R.D., Campbell, N.E.R., 1974. Measurement of microbial oxidation of methane in lake water. Limnol. Oceanogr. 19, 519–524.

Saad, O.A.L.O., Conrad, R., 1993. Temperature dependence of nitrification, denitrification, and turnover of nitric oxide in different soils. Biol. Fert. Soils 15, 21–27.

Sivan, O., Adler, M., Pearson, A., Gelman, F., Bar-Or, I., John, S.G., Eckert, W., 2011. Geochemical evidence for iron-mediated anaerobic oxidation of methane. Limnol. Oceanogr. 56, 1536–1544.

SPW-DGO3, 2015. Etat des nappes d'eau souterraine de Wallonie. Belgique.

Tang, K.W., McGinnis, D.F., Frindte, K., Brüchert, V., Grossart, H.-P., 2014. Paradox reconsidered: methane oversaturation in well-oxygenated lake waters. Limnol. Oceanogr. 59, 275–284.

Tang, K.W., McGinnis, D.F., Ionescu, D., Grossart, H.-P., 2016. Methane production in oxic lake waters potentially increases aquatic methane flux to air. Environ. Sci. Technol. Lett. 3, 227–233.

Van Hulle, S.W.H., Vandeweyer, H.J.P., Meesschaert, B.D., Vanrolleghem, P.A., Dejans, P., Dumoulin, A., 2010. Engineering aspects and practical application of autotrophic nitrogen removal from nitrogen rich streams. Chem. Eng. J. 162, 1–20.

Weiss, R.F., 1981. Determinations of carbon dioxide and methane by dual catalyst flame ionization chromatography and nitrous oxide by electron capture chromatography. J. Chromatogr. Sci. 19, 611–616.

Weiss, R.F., Price, B.A., 1980. Nitrous oxide solubility in water and seawater. Mar. Chem. 8, 347–359.

Westwood, D., 1981. Ammonia in Waters. Methods for the Examination of Waters and Associated Materials. HMSO, London, United Kingdom.

Yamamoto, S., Alcauskas, J.B., Crozier, T.E., 1976. Solubility of methane in distilled water and seawater. J. Chem. Eng. Data 21, 78–80.